

**Egor A. Dyukarev<sup>\*1,2</sup>, Evgeniy A. Godovnikov<sup>1</sup>, Dmitriy V. Karpov<sup>1</sup>, Sergey A. Kurakov<sup>2</sup>, Elena D. Lapshina<sup>1</sup>, Ilya V. Filippov<sup>1</sup>, Nina V. Filippova<sup>1</sup>, Evgeniy A. Zarov<sup>1</sup>**

<sup>1</sup>Yugra State University, Khanty-Mansiysk, Russia

<sup>2</sup>Institute of Monitoring of Climatic and Ecological System of the Siberian Branch Russian Academy of Sciences, Tomsk, Russia

\* **Corresponding author:** dekot@mail.ru

# NET ECOSYSTEM EXCHANGE, GROSS PRIMARY PRODUCTION AND ECOSYSTEM RESPIRATION IN RIDGE-HOLLOW COMPLEX AT MUKHRINO BOG

**ABSTRACT.** The continuous field measurements of net ecosystem exchange (NEE) of CO<sub>2</sub> were provided at ridge-hollow oligotrophic bog in the Middle Taiga Zone of West Siberia, Russia in 2017-2018. The model of net ecosystem exchange of CO<sub>2</sub> was suggested to describe the influence of different environmental factors on NEE and to estimate the total carbon budget of the bog over the growing season. The model uses air and soil temperature, incoming photosynthetically active radiation (PAR) and water table depth, as the key factors influencing gross primary production (GPP) and ecosystem respiration (ER). The model coefficients were calibrated using the data collected by automated soil CO<sub>2</sub> flux system with two transparent long-term chambers placed at large hollow and small ridge sites.

Experimental and modeling results showed that the Mukhrino bog acted over the study period as a carbon sink, with an average NEE of  $-87.7 \text{ gC m}^{-2}$  at the hollow site and  $-50.2 \text{ gC m}^{-2}$  at the ridge site. GPP was  $-344.8$  and  $-228.5 \text{ gC m}^{-2}$  whereas ER was  $287.6$  and  $140.9 \text{ gC m}^{-2}$  at ridge and hollow sites, respectively. Despite of a large difference in NEE estimates between 2017 and 2018 the growing season variability of NEE were quite similar.

**KEY WORDS:** carbon dioxide, net ecosystem exchange, peatlands, ridge-hollow complex, ecosystem respiration, gross primary production

**CITATION:** Egor Dyukarev, Evgeniy Godovnikov, Dmitriy Karpov, Sergey Kurakov, Elena Lapshina, Ilya Filippov, Nina Filippova, Evgeniy Zarov (2019) Net Ecosystem Exchange, Gross Primary Production And Ecosystem Respiration In Ridge-Hollow Complex At Mukhrino Bog. *Geography, Environment, Sustainability*, Vol.12, No 2, p. 227-244  
DOI-10.24057/2071-9388-2018-77

## INTRODUCTION

Peatland ecosystems play a significant role in the global carbon cycle, being sources and sinks of greenhouse gases (GHG) (Ciais et al. 2013; Rydin and Jeglum 2015). Despite covering a relatively small part of the Earth surface (about 3%), peatlands store a large amount of organic matter that is ranged between 500 and 700 billion tonnes of C (Page and Baird 2016; Leifeld and Menichetti 2018). In West Siberia peatlands occupy over 30% of the area (Terentieva et al. 2016; Dyukarev et al. 2011; Sheng et al. 2004). According to IPCC estimates (Ciais et al. 2013) the contribution of natural mires into total natural methane emissions ranged between 61 and 82%. The intensity of GHG fluxes is controlled by different factors including the hydrological and thermal regime of the peat deposit (Naumov 2009; Sasakawa et al. 2012; Helfter et al. 2015; Molchanov 2015; Walker et al. 2016; Glagolev et al. 2017; Veretennikova and Dyukarev 2017; Leroy et al. 2017).

The gaseous exchange between the atmosphere and the peatlands is governed by photosynthetic fixation of  $\text{CO}_2$  from the atmosphere and by soil and vegetation respiration losses of  $\text{CO}_2$ . The balance between them is known as the net ecosystem exchange (NEE) of  $\text{CO}_2$  (Bubier et al. 2003; Olchev et al. 2009; Golovatskaya and Dyukarev 2012; Helfer et al. 2015). The other major gaseous emission of C into the atmosphere is accounts for methane ( $\text{CH}_4$ ), which is produced via anoxic decay of the soil organic matter (Saunois et al. 2016). The loss of C into the fluvial system occurs via export of dissolved and particulate organic carbon, and dissolved gases ( $\text{CO}_2$  and  $\text{CH}_4$ ). The rise in surface air temperature (Zhaojun et al. 2011; Baird et al. 2012) and the lowering of water levels causes peat drying, increase of temperature and aeration, which contributes to the intense of greenhouse gas emissions (Baird et al. 2012; The second assessment report... 2014). Peatland ecosystems in different years can also serve as both a source and a sink of carbon (Golovatskaya et al. 2008; Panzaoo et al. 2017). The variety of direct and inverse relationships existing

between the components of the peatlands and the surrounding areas indicates a complex nonlinear impact of peatlands on the environment in different geographic, climatic, and geomorphological conditions (Peatlands of West Siberia 1976; Vomperskiy 1994; Ratcliffe et al. 2017; Webster et al. 2018). The quantitative estimation of the rate of carbon exchange between peatlands and the atmosphere, as well as the revealing of environmental factors affecting carbon exchange, is an important scientific issue (Sheng et al. 2004; Kabanov 2015).

High-precision measurements of carbon and GHG fluxes obtained using standardised methodologies are important for our understanding C cycle within and across ecosystems. (see Franz et al. 2018; Pavelka et al. 2018). The study of the hydrological and ecological mechanisms controlling peatland response to climate changes is critical to predict potential feedbacks on the global C cycle (Baird et al. 2012; The second assessment report... 2014). Recent field studies indicated that the peatland C balance represents a net C sink in intact peatlands in Canada (Wu et al. 2010; Munir et al. 2014; Webster et al. 2018), China (Zhu et al. 2015; Zhou et al. 2009), Finland (Laine et al. 2019; Minkinen et al. 2018), Ireland (Swenson et al. 2019), Scotland (Helfter et al. 2015), Germany (Günther et al. 2017), France (Leroy et al. 2017), Poland (Acosta et al. 2017), New Zealand (Campbell et al. 2014), East (Runkle et al. 2013; Fleischer et al. 2016; Eckhardt et al. 2018; Davydov et al. 2018) and Western part of Russia (Kurbatova et al. 2009; Kurganova et al. 2011; Molchanov 2015; Ivanov et al. 2017).

Modelling approaches are useful to divide the observed NEE into gross primary production (GPP) and total ecosystem respiration (ER) components, since it provides a better diagnostic of ecosystem processes and their regulating factors (Falge et al. 2001; Widlowski et al. 2011). Carbon balance models are used to quantify the contribution of different environmental factors to GPP, ER and NEE variability, and to calculate daily and annual carbon bud-

gets using the gap-filled time series. Partitioning of the NEE into GPP and ER is also needed for better understanding of inter-annual and spatial variability of the carbon fluxes (Sokolov et al. 2019). The fundamental ecosystem processes (including photosynthesis and respiration) are common to mires and other terrestrial ecosystems, so changes in photosynthetically active radiation (PAR), air temperature ( $T_a$ ), and precipitation may affect the C cycle in peatlands, e.g. due to alterations of the growing season length, water and energy budget, vegetation composition and water table levels (WTL) (Yurova et al. 2007; Humphreys and Lafleur 2011, Grant et al 2012, Campbell et al. 2014; Molchanov and Olchev 2016; Eckhardt et al. 2018).

The main purpose of this study is to assess  $CO_2$  exchange fluxes in oligotrophic peatland complex at the Middle Taiga Zone in West Siberia using field chamber measurements and developed mathematical model of NEE.

## MATERIALS AND METHODS

The field measurements were provided on the international scientific field station “Mukhrino” (Yugra State University, Khanty-Mansijsk) founded in 2009 (Lapshina et al. 2015). The field station is a part of the International Network for Terrestrial Research and Monitoring in the Arctic (INTERACT, eu-interact.org) and is actively used by Russian and foreign scientists for studies of the functioning of mire ecosystems. Over the past years, the Mukhrino bog was the main object of numerous experimental study of GHG fluxes (Glagolev et al. 2011; Alekseychik et al. 2017), geochemistry and physical, chemical, and biochemical properties of peat (Stepanova and Pokrovsky 2011; Szajdak et al. 2016), mire hydrology (Bleuten and Filippov 2008), and microbiology including mycology (Filippova et al. 2015).

The Mukhrino bog (60°54'N, 68°42'E) is located at the eastern terrace of the Irtysh River 20 km to the south from the point of its confluence with the Ob River, in the middle taiga zone of the West Siberian

Lowland (Alekseychik et al. 2017). The climate of the region is a subarctic or boreal (Dfc) according to Köppen–Geiger climate classification with long cold winters and short warm summers. Mean annual temperature at Khanty-Mansijsk weather station for period 1983–2013 is  $-0.7^\circ C$ , annual precipitation is 526 mm, sunshine duration is 1845 hours (Grebenuk and Kuznetsova 2012).

Pine bogs and ridge–hollow complexes are dominant at the boundaries of the Mukhrino peatbog. The vegetation is represented by rare pine trees and shrubs, dense herbaceous vegetation and mosses. Tree cover is mainly represented by stunted *Pinus sylvestris*. The dwarf shrub layer consists of *Ledum palustre*, *Andromeda polifolia*, *Chamaedaphne calyculata*, *Vaccinium vitis-idaea*, *Vaccinium uliginosum*, and *Oxycoccus palustris*. Herbs are represented by *Rubus chamaemorus* and a few tiny species of sundews (*Drosera anglica*, *D. intermedia*, *D. rotundifolia*). *Carex limosa*, *Eriophorum vaginatum*, *Scheuchzeria palustris* are widespread within oligotrophic hollows of ridge–hollow complexes. The moss layer consists of sphagnum mosses such as *S. fuscum*, *S. lindbergii*, *S. balticum*, *S. papillosum*, *S. angustifolium*, *S. magellanicum*, *S. jensenii*, etc. The area fractions of open water, hollows, and ridges within a 200 m radius around the observation site are 1, 67, and 32% (Alekseychik et al. 2017). Automated monitoring of carbon dioxide fluxes at oligotrophic ridge–hollow complex was performed in 2017–2018 using the portable atmospheric soil measuring system (ASMS) with two transparent chambers. Automated chambers were placed at a large hollow and a small ridge. ASMS is able to measure and record simultaneously the following environmental parameters: air temperature ( $T_a$ ) and humidity (RH) (at height of 2 m above the ground and at the ground surface), PAR (incoming solar radiation in the 400–700 nm spectral range), carbon dioxide content and water vapor pressure in the air samples. The system includes a two-channel gas analyzer Li-7000 (Li-COR Biogeosciences, USA) and two measuring chambers with a volume of 120 l. The chambers are closed for 5

minutes every hour (or 3 hours in 2017) to provide the flux measurement. The rest of the time they remain open. The air for a sample is continuously pumped through the chamber and the gas analyzer during the observation period using diaphragm pump 7006ZVR (Gardner Denver Thomas GmbH, Germany) with flow rate about 2 l/minute. The measurements of the concentration of CO<sub>2</sub> and H<sub>2</sub>O, Ta, RH and PAR are continuously stored in the ASMS and transferred to the web-server. The observation data were downloaded from server and processed using specially created software modules. Real-time ground water depth monitoring was conducted using a pressure transducer (Mini-diver DL501, Van Essen Instruments, Netherlands) submerged into a water at a fixed level under the surface.

The automated system operated in a measuring mode from July to August in 2017, and from May to October in 2018. The flux of CO<sub>2</sub> was calculated using a specialized software module developed in the Matlab R2014b (MathWorks, USA) using a linear model for changing the concentration in the chambers during the first two minutes of data sampling. Totally about 500 observations of fluxes were made at each experimental site in 2017 and more than 2500 observations - in 2018, respectively.

**Mathematical modelling**

To obtain continuous data records, to extrapolate them to other periods when experimental data are missing and to calculate the annual carbon budget of the ecosystem, a model of total ecosystem

carbon exchange was proposed (Dyukarev 2017). The measured total NEE (Fig.1) was partitioned into the incoming (GPP) and expenditure (ER) components (Mäkelä et al. 2004; Laine et al. 2009; Kandel et al. 2013; Campbell et al. 2015).

$$NEE = ER - GPP; \tag{1}$$

$$GPP = f_w \times f_{PAR}; \tag{2}$$

$$ER = f_w \times f_T; \tag{3}$$

GPP is defined as the total amount of the carbon fixed in the process of photosynthesis by plants in an ecosystem, while NEE refers to GPP minus ER. ER is the result of plants and soil respiration, where soil respiration is the sum of autotrophic respiration (roots) and heterotrophic respiration (soil biota).

It is well known that the photosynthetic response under low light intensities is characterized by a linear response and photosynthetic saturation is observed at high light intensities (Pessaraki 2005). A rectangular hyperbolic function  $f_{PAR}$  (4) is used for the light response of NEE in daytime (Mäkelä et al. 2004; Laine et al. 2009).

$$f_{PAR} = \alpha \times PAR \times G_m / (\alpha \times PAR + G_m); \tag{4}$$

where  $\alpha$  is the initial slope of the light response curve at low light (photosynthetic efficiency) ( $mg \mu mol^{-1}$ ),  $G_m$  is the theoretical maximum rate of photosynthesis at infinite PAR (photosynthetic capacity) ( $mg m^{-2} h^{-1}$ ). Carbon dioxide fluxes are given in  $mg$  of CO<sub>2</sub> per m<sup>2</sup> per hour. PAR is measured in  $\mu mol m^{-2} s^{-1}$ . Possible GPP limitation at high air temperatures was not accounted.

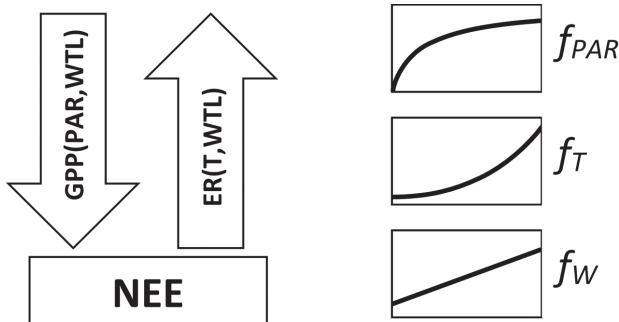


**Fig. 1. Schematic representation of CO<sub>2</sub> fluxes (1-3) and shapes of environmental response curves (4-5)**

The total ecosystem respiration was modelled using an exponential equation  $f_T$  (5) widely used for explanation of ER variation (Kandel et al. 2013; Campbell et al. 2015). The shapes of functional dependence of C fluxes from environmental variables are shown in Fig. 1.

$$f_T = E_0 \times \exp(k_T \times T_a); \quad (5)$$

where  $T_a$  is air temperature ( $^{\circ}\text{C}$ ),  $E_0$  is the reference ecosystem respiration ( $\text{mg m}^{-2} \text{h}^{-1}$ ) at  $T_a = 0^{\circ}\text{C}$  and  $WTL = 0$ ,  $k_T$  is coefficient describing the respiration temperature response ( $^{\circ}\text{C}^{-1}$ ).

The rate of photosynthesis and respiration of *Sphagnum* mosses are well correlated with peat moisture (Molchanov and Olchev 2016; Taylor et al. 2016). Changes in water table depth strongly influence GPP (Grant et al. 2012; Pugh et al. 2018), ER (Helfter et al. 2015), and heterotrophic respiration (Eckhardt et al. 2018). Additional factor  $f_W$  (6) characterises the influence of WTL on GPP and ER fluxes and can be expressed in a simple linear form:

$$f_W = 1 + k_W \times WTL; \quad (6)$$

where  $k_W$  is a parameter of sensitivity of GPP and ER to variation of WTL ( $\text{cm}^{-1}$ ).

NEE is negative when the value of GPP exceeds the ER value and there is a net removal of carbon dioxide from the atmosphere. NEE is positive when the ER value exceeds the GPP value and the carbon dioxide is released from the ecosystem into the atmosphere.

The model has been calibrated using all available data set on carbon dioxide fluxes in 2017 and 2018. Two-step procedure of model calibration was developed to estimate model parameters. At the first step, model parameters were calculated for each studied site (ridge and hollow) using all the available data for 2017-2018. At the second step,  $k_T$ ,  $G_{max}$ ,  $k_W$  were fixed and the  $E_0$  and  $a$  were calculated for each month of the study period separately. Multi-objective optimization procedure was performed in the Matlab software using

*fminsearch* function. The minimum of the unconstrained multivariable function was found using derivative-free optimization method (Lagarias et al. 1998). Root-mean-square error was used as a minimizing function (Dyukarev 2017).

## RESULTS AND DISCUSSION

### Environmental conditions

During the study period (May – October 2017 and 2018) environmental conditions characterized by large seasonal and diurnal variability (Fig. 2). Minimum air temperature ( $-7.4^{\circ}\text{C}$ ) was observed at 4:00 a.m. (local time) on October 23, 2018. Maximum value the air temperature ( $+32.3^{\circ}\text{C}$ ) reached at 14:00 on July 12, 2018. Rapid temperature raise with a daily mean temperature above  $10^{\circ}\text{C}$  occurs after June 1. The monthly mean air temperature of June 2017 was  $16.4^{\circ}\text{C}$ , the mean air temperature of June 2018 was  $14.2^{\circ}\text{C}$ . Monthly air temperatures in 2018 were slightly lower than in 2017, except July and October. July air temperatures were  $18.3^{\circ}\text{C}$  and  $19.1^{\circ}\text{C}$  in 2017 and 2018, respectively. October 2018 was extremely warm with mean air temperature  $3.9^{\circ}\text{C}$ , when mean temperature in October 2017 was  $0^{\circ}\text{C}$ .

The maximal values of incoming PAR (up to  $1861 \mu\text{mol m}^{-2} \text{s}^{-1}$ ) were observed in the middle of a day (at 11:00 on June 26, 2018). Daily maximal incoming solar radiation increased from May to mid-June. Mean monthly PAR in June were  $1384$  and  $1571 \mu\text{mol m}^{-2} \text{s}^{-1}$  in 2017 and 2018, respectively. Minimal PAR values were observed in October:  $355$  and  $425 \mu\text{mol m}^{-2} \text{s}^{-1}$  for 2017 and 2018, respectively. The daily averaged PAR in May-July in 2017 were somewhat higher than in 2018, whereas the daily PAR in August-October were higher in 2018 than in 2017.

The depth of the water table level is gradually decreased from the early spring after snowmelt to the end of summer (Fig. 2). Rapid rise of WTL occurs after heavy rains. The total amount of precipitation over the growing season in 2018 ( $315 \text{ mm}$ ) was higher than in 2017 ( $288 \text{ mm}$ ) and it is resulted in higher WTL in 2018.

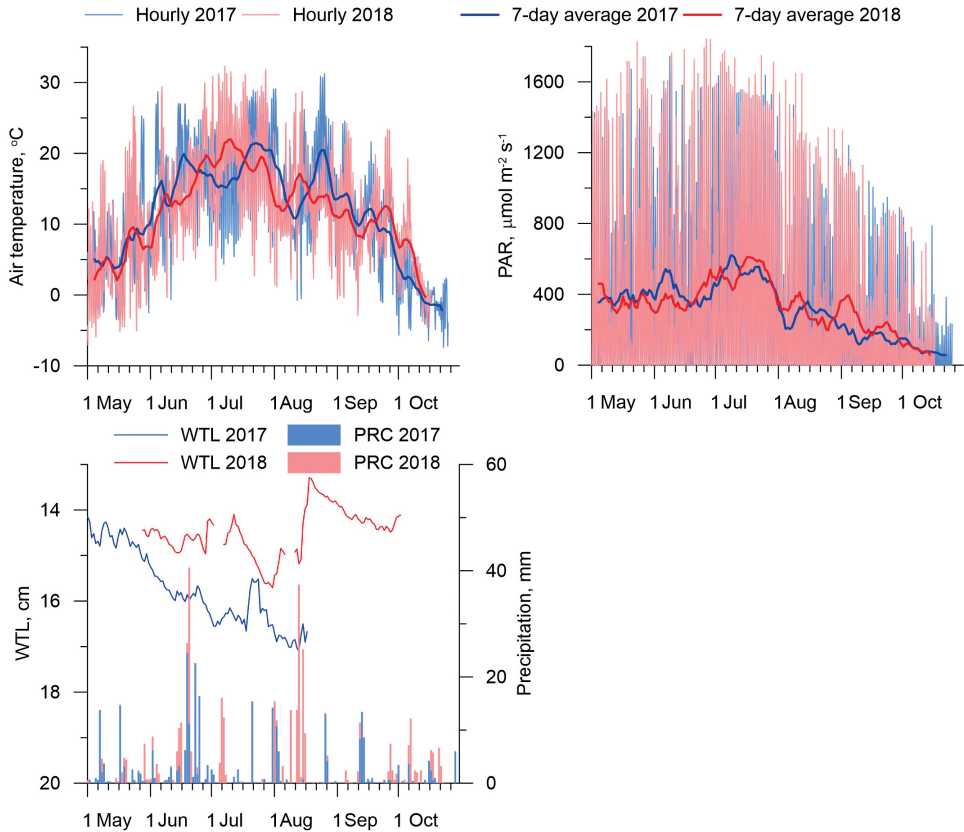


**Fig. 2. Seasonal variations of the air temperature ( $T_a$ ), photosynthetically active radiation (PAR), water table level (WTL) and precipitation (PRC) in May-October 2017 and 2018. Thin lines show hourly data, bold lines show 7-days running average values**

### Carbon dioxide fluxes

Monthly averaged diurnal variations of the  $\text{CO}_2$  fluxes for different months and their standard deviations are shown in Fig.3. A diurnal course of fluxes is quite similar for entire period of measurements. The daily pattern of carbon dioxide fluxes is characterized by a clear maximum at night hours (from 11 p.m. to 1 a.m.) when  $\text{CO}_2$  is released into the atmosphere, and minimum from 10 a.m. to 1 p.m., when  $\text{CO}_2$  uptake by plants exceeds the ecosystem respiration (Golovatskaya, Dyukarev, 2011). Night hours are characterized by positive fluxes whereas negative fluxes are observed from early morning (4 – 6 a.m.) until late evening (6 – 8 p.m.).

The NEE rate changed the sign from positive (release) to negative (uptake) in May even at low air temperatures and remained

in the time at relatively low level.  $\text{CO}_2$  fluxes increased during the first half of summer whereas GPP and ER reached maximum values at mid-July. ER in August-October is lower than in mid-summer due to decreased air and soil temperatures, but it is higher than at the beginning of the growing season because of a large amount of plant litter and mortmass.

The diurnal pattern of measured  $\text{CO}_2$  fluxes on the hollow site in different summer months of 2017, does not vary significantly (Fig. 3). The ridge site is characterized in turn by a slightly decreased  $\text{CO}_2$  absorption before noon and increased nocturnal emission from June to August. The early spring in 2017 resulted in a long growing season and, consequently, early onset of the development of vascular plants.

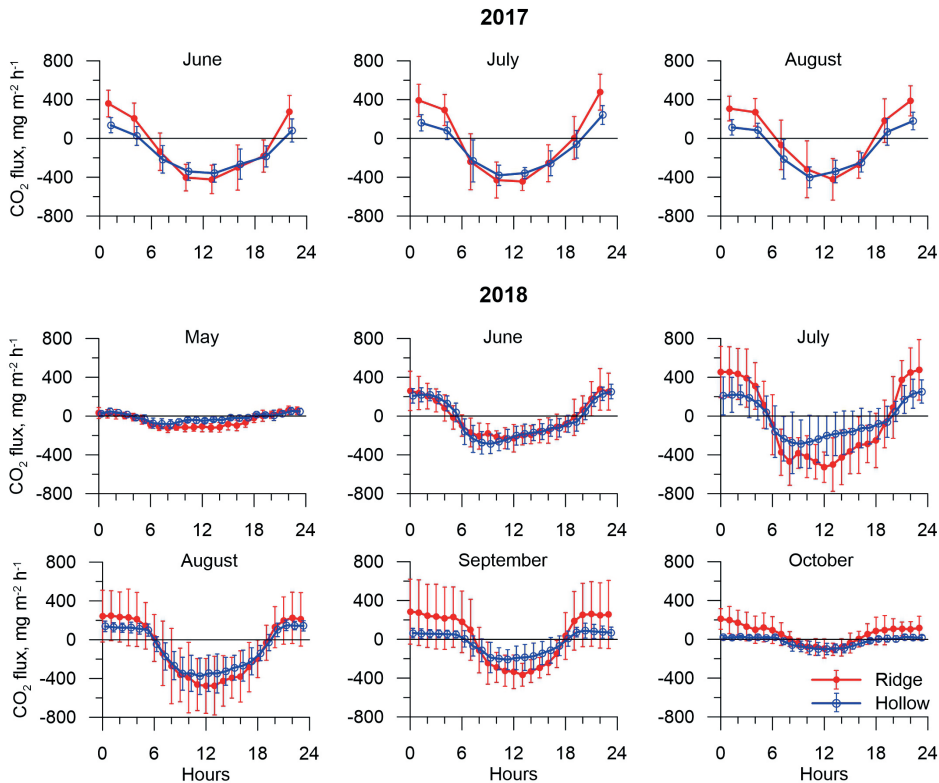


**Fig. 3. Monthly averaged diurnal variations of CO<sub>2</sub> fluxes measured at ridge and hollow sites at Mukhrino bog in June–August 2017 and May–October 2018. (Dots – average values, vertical whiskers – standard deviations)**

Maximal diurnal variation of fluxes is typical for July, when diurnal range of the fluxes reached 622 and 1004 mg m<sup>-2</sup> h<sup>-1</sup> at hollow and ridge sites, respectively. In May and October 2018, diurnal dynamics of fluxes was very smoothed and characterized by lowered diurnal amplitude. The amplitude of diurnal variations of the CO<sub>2</sub> fluxes in September was 127 and 313 mg m<sup>-2</sup> h<sup>-1</sup> at hollow and ridge sites, respectively.

Dwarf shrubs and herbs available at the ridge site are characterized by higher green biomass than sedge at the hollow site. Therefore, both CO<sub>2</sub> uptake and emission fluxes at the ridge site have higher absolute NEE values during the entire growing season, excepting May.

Obtained results are well agreed with measured fluxes at peatlands in other geographical regions. In particular, NEE at peatbog in the south taiga in the European

part of Russia (Ivanov et al., 2017) in summer period 2014 was positive (+200 mg m<sup>-2</sup> h<sup>-1</sup>) at hummocks and negative (-79 mg m<sup>-2</sup> h<sup>-1</sup>) at hollow sites. Under very dry and hot weather conditions in year 2015, CO<sub>2</sub> balance in hummock and hollow was positive with NEE reached +220 and +31 mg m<sup>-2</sup> h<sup>-1</sup>, respectively. Ecosystem respiration was significantly higher (300–700 mg m<sup>-2</sup> h<sup>-1</sup>) than the ER rates obtained in our study. According to our estimates, CO<sub>2</sub> emission at the ridge site was 2–4 times higher in comparison with estimations in a forested peatbog of the southern taiga in West Siberia (Golovatskaya and Dyukarev 2012). NEE measured in a patterned peatland in Ireland (Laine et al., 2006) have showed, that the absolute flux rates were some higher at hummocks and lower at hollows. The daytime average NEE at the sites were -1700 and -330 mg m<sup>-2</sup> h<sup>-1</sup> at hummock and hollow; and the average night time fluxes were +300 and +50 mg m<sup>-2</sup> h<sup>-1</sup>, respectively.

## Model calibration

The adequate projection of carbon cycle by an ecosystem-level model requires accurate calibration of model input parameters (Wu et al. 2010). The NEE rate measured by automated system was partitioned into ecosystem respiration ER and GPP using suggested NEE model. At the first step of the model calibration all available observation data for the years 2017 and 2018 were used. The 3299 and 3190 observations were used in total for each experimental site (ridge and hollow).

The results of calibration showed a great difference between key model parameters for both experimental sites. The temperature sensitivity coefficient ( $k_T$ ) for ER rate for the ridge site was about two times smaller than for the hollow site, but at the same time the reference respiration ( $E_0$ ) at the ridge site was 5.4 times higher (Table 1). The photosynthetic efficiency ( $\alpha$ ) and photosynthetic capacity ( $G_m$ ) obtained for the ridge site were about 1.7 times higher than corresponding parameter for the hollow site, likely due to difference in green biomass amount. The effect of WTL on  $\text{CO}_2$  fluxes at the hollow site was higher comparing with the ridge site. The model calibrated for the whole data set allows reproducing adequately the fast diurnal variations of  $\text{CO}_2$  fluxes, but the projected diurnal variations are significantly lower than

the variation obtained from observation data. Mean error (difference between modeled and observed data) was small resulting in high correlation between simulated and observed fluxes ( $R > 0.94$ ,  $R^2 > 0.84$ , significant at  $p < 0.05$ ), although the mean absolute error (MAE) was quite high (Table 1).

In the second step of the model calibration,  $k_T$ ,  $G_m$  and  $k_W$  were taken to be constant and equal to the values obtained after the first calibration step (Table 2). The parameters  $E_0$  and  $\alpha$  were calculated for each month of the study period separately. The number of observations used for model calibration varies from 110 in June 2017 to 661 in September 2018.

The parameters  $\alpha$  and  $E_0$  increase during the growing season simultaneously with plant biomass development until the mid-summer (Table 2). The maximum values of photosynthetic efficiency ( $5.14 \text{ mg } \mu\text{mol}^{-1}$ ) were obtained for July 2018 at the ridge site. The maximum values of  $\alpha$  for the hollow site were by 20-60% lower than for the ridge. Seasonal course of photosynthetic efficiency is well pronounced and  $\alpha$  value for May is significantly lower than  $\alpha$  value for middle of the growing season, and about two times lower than the value for the end of the season (October).

**Table 1. Calibration step 1. NEE model parameters for ridge and hollow sites. (n - number of observations,  $G_m$ ,  $\alpha$ ,  $k_T$ ,  $E_0$ ,  $k_W$  - model parameters,  $R^2$  - determination coefficient, ME - mean error, MAE - mean absolute error)**

	Ridge	Hollow
$n$	3299	3190
$G_m, \text{mg m}^{-2} \text{h}^{-1}$	885.4	548.9
$\alpha, \text{mg } \mu\text{mol}^{-1}$	2.08	1.13
$k_T, ^\circ\text{C}^{-1}$	0.038	0.091
$E_0, \text{mg m}^{-2} \text{h}^{-1}$	126.3	23.5
$k_W, \text{cm}^{-1}$	0.01	0.03
$R^2$	0.85	0.84
ME, $\text{mg m}^{-2} \text{h}^{-1}$	-5.99	-7.92
MAE, $\text{mg m}^{-2} \text{h}^{-1}$	65.0	42.3



**Table 2. Calibration step 2. NEE model parameters for ridge and hollow sites (*n* - number of observations, *a*, *E<sub>0</sub>* - model parameters, MAE - mean absolute error)**

		Ridge				Hollow			
		<i>n</i>	<i>a</i> , mg μmol <sup>-1</sup>	<i>E<sub>0</sub></i> , mg m <sup>-2</sup> h <sup>-1</sup>	MAE, mg m <sup>-2</sup> h <sup>-1</sup>	<i>n</i>	<i>a</i> , mg μmol <sup>-1</sup>	<i>E<sub>0</sub></i> , mg m <sup>-2</sup> h <sup>-1</sup>	MAE, mg m <sup>-2</sup> h <sup>-1</sup>
2017	June	110	3.31	189.9	25.8	110	1.78	32.9	16.5
	July	204	3.71	190.0	31.1	201	1.79	24.8	30.5
	August	183	2.46	164.2	21.5	161	1.65	28.3	28.0
2018	May	220	0.19	17.6	16.8	209	0.08	7.7	19.5
	June	535	0.94	111.9	36.3	523	0.75	30.1	24.3
	July	545	5.14	186.1	27.8	490	3.11	36.2	21.9
	August	558	2.45	116.8	33.1	561	1.90	33.2	16.1
	September	661	2.36	146.6	35.2	655	0.61	20.7	14.8
	October	253	0.73	75.5	25.6	250	0.33	8.4	10.6
Projected parameters									
2017	May	–	0.63	56.4	–	–	0.27	11.7	–
	September	–	1.19	87.4	–	–	0.57	17.4	–
	October	–	0.23	27.7	–	–	0.08	6.2	–

The ER rate growth is mainly influenced by increased autotrophic respiration rates due to raised biomass amount and increased soil temperatures. *E<sub>0</sub>* for the hollow site was significantly smaller than the value at the ridge site due to lower biomass amount and reduced contribution of leaf and root respiration.

The model parameters *a* and *E<sub>0</sub>* for ridge and hollow sites were related with monthly air temperature *T<sub>m</sub>* using exponential model:

$$a(\text{Ridge}) = 0.22 \exp(0.16 \times T_m), R^2 = 0.69;$$

$$a(\text{Hollow}) = 0.08 \exp(0.19 \times T_m), R^2 = 0.79;$$

$$E_0(\text{Ridge}) = 27.15 \exp(0.11 \times T_m), R^2 = 0.61;$$

$$E_0(\text{Hollow}) = 6.06 \exp(0.10 \times T_m), R^2 = 0.82.$$

These equations were used for projection of *a* and *E<sub>0</sub>* for May, September and October 2017 taking into account monthly air temperatures (Table 2).

### Monthly CO<sub>2</sub> fluxes

Time series of gap-filled modeled ER, GPP and NEE fluxes were integrated for each month of the study period. Annual variability of monthly carbon fluxes for ridge and hollow sites is shown in Fig 4. The largest ER efflux was measured in July 2017 at the ridge site - 97.3 gC m<sup>-2</sup>. Respiration rate at the hollow site reached maximum values in July too, and they were somewhat lower than at the ridge site - 42.1 gC m<sup>-2</sup>. In May, the total respiration at both sites were similar and does not exceed 17.9 gC m<sup>-2</sup> in 2018 and 5.6 gC m<sup>-2</sup> in 2017 because of lower temperatures. June and August were characterized by moderate respiration fluxes ranging between 13.8 and 75.0 gC m<sup>-2</sup>. The more intense emission was obtained for the ridge site where various vascular species strongly contribute to autotrophic part of respiration and thicker acrotelm layer promotes aerobic

decomposition of plant residuals. The ER rate in September and October was still high at the ridge site but because of low GPP the ridge acted as a source of CO<sub>2</sub> for the atmosphere.

The recovery of photosynthetic activity of peatbog vegetation began in 2017 in early spring and the GPP rate reached rather high values in May – 20.7 and 43.4 gC m<sup>-2</sup> for hollow and ridge sites, respectively. Due to late spring in 2018 the GPP values in May was essentially lower for both sites – 2.7 and 7.1 gC m<sup>-2</sup> for hollow and ridge sites, respectively. GPP reached its maximum rates in July – 120.3 gC m<sup>-2</sup> at the ridge site and 91.3 gC m<sup>-2</sup> at the hollow site. June and August of 2017 and 2018 are characterized by lower values of GPP because of lower PAR values (see Fig.2). The hollow site is characterized by faster autumn decrease of GPP comparing with ridge site.

The ratio of GPP to ER is used to estimate the fraction of assimilated carbon that was consumed by the plants (Falge et al., 2002). Analysis of the GPP/ER ratio for the entire measuring period showed that the ratio was 1.2 for the ridge site and 1.6 for the hollow site respectively. Both sites acted as a sink of carbon dioxide from the atmosphere.

The largest variations of carbon fluxes were observed at the ridge site, where seasonal

maximums in absolute values of ER and GPP significantly exceed the corresponding values at the hollow site. The hollow site has smoother fluxes dynamics and lower absolute values of ER and GPP. Despite of the found differences in GPP and ER between both sites, monthly NEE was higher at the hollow site. Summer month rates of NEE at the hollow site varied from -0.3 to -40.7 gC m<sup>-2</sup> in 2017 and from +0.5 to -27.0 gC m<sup>-2</sup> in 2018, whereas at the ridge site NEE changed from +1.8 to -25.4 gC m<sup>-2</sup> in 2017 and from +14.0 to -23.5 gC m<sup>-2</sup> in 2018. The maximal carbon uptake occurred in July at both sites. Small positive NEE values (up to 14.0 gC m<sup>-2</sup>) were obtained for June and October 2018 at the ridge site and for May and June 2018 at the hollow site, respectively.

The growing season cumulative NEE, calculated by integrating the monthly averaged diurnal NEE rates for period from May to September was -78.5 and -121.6 gC m<sup>-2</sup> in 2017 for ridge and hollow sites, respectively. Results show that amount of captured CO<sub>2</sub> from the atmosphere for both experimental sites was lower for year 2018 than for the same period in 2017. While the cumulative NEE rate for ridge site was -21.9, for hollow site it reached -53.8 gC m<sup>-2</sup>. The most significant decrease in NEE at the hollow site from 2017 to 2018 occurs mainly due to decrease in GPP from 257.3 to 199.8 gC m<sup>-2</sup>, and insignificant rise in ER rates from 135.7 to 146.0 gC m<sup>-2</sup>. High-

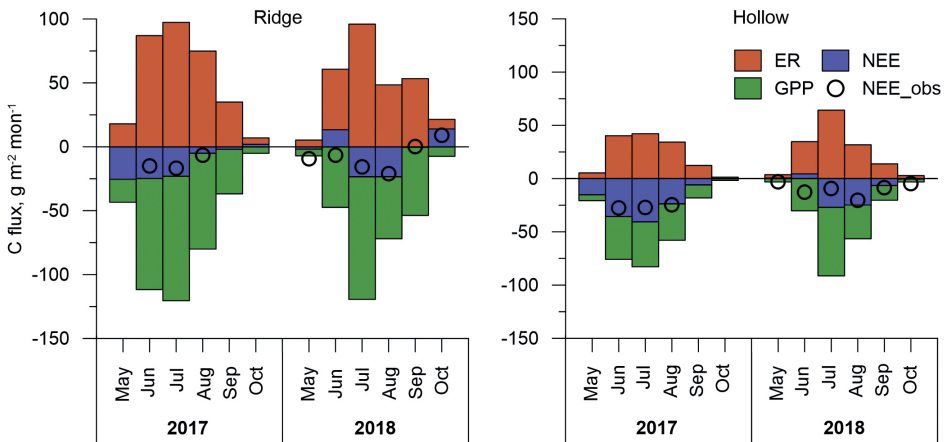


**Fig. 4. Monthly carbon dioxide fluxes at the ridge and hollow sites at Mukhrino bog in 2017 and 2018. Circles show NEE observations, bars – model estimations for ER, GPP and NEE**

er values of NEE in 2018 at the ridge site were obviously related with smaller values of the both GPP and ER rates. Whereas ER rate at the ridge site decreased from 317.3 to 257.9 gC m<sup>-2</sup>, GPP falls down from 395.8 to 293.8 gC m<sup>-2</sup>.

Over the two years of flux measurements, the average annual uptake of CO<sub>2</sub> was 87.7 gC m<sup>-2</sup> at the hollow and 50.2 gC m<sup>-2</sup> at the ridge site at Mukhrino bog and the NEE rates were quite similar to findings at other peatland sites. In particular, two years of measurements of CO<sub>2</sub> fluxes in the Stordalen palsa mire (a nutrient poor permafrost peatland) in Sweden showed that the mire was a net sink of carbon, with average annual uptake of -46 gC m<sup>-2</sup> per year (Olefeldt et al. 2012). The results of two years flux measurements in a boreal minerogenic oligotrophic mire in northern Sweden (Nilsson et al., 2008) showed the peatbog was also a net carbon sink with annual net uptake of about -55 gC m<sup>-2</sup>. McVeigh et al. (2014) reported about the average 10-years annual CO<sub>2</sub> uptake of -55.7 ± 18.9 gC m<sup>-2</sup> in Atlantic blanket bog in Glencar, southwest Ireland. The results of 11 year flux measurements in a temperate lowland peatland in central Scotland (Helfter et al. 2015) showed a very high variation of annual NEE rate that is ranged between -5.2 and -36.9 gC m<sup>-2</sup> yr<sup>-1</sup>.

The differences in microtopographic features between hummocks and hollows and its statistically significant influence on the total ER, but not on GPP, were found by Wu et al. (2010) at ombrotrophic MerBlue bog. NEE rates estimated at the hummock and hollow sites were -66 ÷ +19 gC m<sup>-2</sup> yr<sup>-1</sup> and -146 ÷ -260 gC m<sup>-2</sup> yr<sup>-1</sup>, respectively. The chamber estimates of NEE at patterned blanked bog (Laine et al. 2006) found that the annual NEE of the driest peatbog sites was about 130% larger than the NEE rate at the wet sites, indicating a

large spatial variation that can be found in NEE rates within a quite uniform peatbog ecosystem.

## CONCLUSION

The results of field measurements of CO<sub>2</sub> fluxes at ridge-hollow complex bog in combination with suggested mathematical model allowed us to estimate adequately the NEE, ER and GPP rates for ridge and hollow sites at oligotrophic bog in Middle Taiga Zone of West Siberia. The cumulative CO<sub>2</sub> uptake rates exceed cumulative respiration rates at both experimental sites. The two year average growing season NEE at the hollow site was 1.7 times higher (87.7 gC m<sup>-2</sup>) than at the ridge site (50.2 gC m<sup>-2</sup>). GPP and ER rates at the ridge site were higher than at the hollow site. The influence of key environmental factors (air temperature, incoming photosynthetically active radiation and water table depth) on CO<sub>2</sub> fluxes at each ecosystem was very different. It is claimed by differences in model parameters describing ER and GPP response to changed ambient characteristics. The suggested NEE model is a promising tool to describe the NEE partitioning into GPP and ER, and to better understand the biogeochemical processes in mire ecosystems in order to find new possibilities to extrapolate the data of local observations to peatland ecosystems of Western Siberia.

## ACKNOWLEDGMENTS

This study was supported by the project AAAA-A17-117013050031-8 and grant 13-01-20/39 of the Yugra State University. The field works at Mukhrino field station was funded by Russian Fund for Basic Researches and Government of the Khanty-Mansiysk Autonomous region according to the research project 18-44-860017. ■

## REFERENCES

- Acosta M., Juszczak R., Chojnicki B., Pavelka M., Havránková K., Lesny J., Krupková L., Urbaniak M., Macháčová K., Olejnik J. (2017). CO<sub>2</sub> Fluxes from Different Vegetation Communities on a Peatland Ecosystem. *Wetlands*, V.37, N.3, pp. 423–435. <https://doi.org/10.1007/s13157-017-0878-4>.
- Alekseychik P., Mammarella I., Karpov D., Dengel S., Terentjeva I., Sabrekov A., Glagolev M., Lapshina E.D. (2017). Net ecosystem exchange and energy fluxes measured with the eddy covariance technique in a western Siberian bog. *Atmos. Chem. Phys.*, V.17, pp. 9333–9345. <https://doi.org/10.5194/acp-17-9333-2017>.
- Baird A., Belyea L., Comas X., Reeve A., Slater L. (2013). Carbon Cycling in Northern Peatlands. *Geophysical Monograph Series*. AGU pp. 297.
- Bleuten W., Filippov I. (2008). Hydrology of mire ecosystems in central West Siberia: the Mukhrino Field Station, in *Transactions of UNESCO department of Yugorsky State University "Dynamics of environment and global climate change"* ed. Lapshina, E. D., Novosibirsk, NSU, pp. 208–224.
- Bubier J.L., Crill P.M., Mosedale A., Frohling S., Linder E. (2003). Peatland responses to varying interannual moisture conditions as measured by automatic CO<sub>2</sub> chambers. *Glob. Biogeochem Cycles*. V.17. N.2, p.1066. <https://doi.org/10.1029/2002GB001946>.
- Campbell D.I., Smith J., Goodrich J.P., Wall A.M., Schipper L.A. (2014). Year-round growing conditions explains large CO<sub>2</sub> sink strength in a New Zealand raised peat bog. *Agricultural and Forest Meteorology*, V.192–193, pp.59–68. <https://doi.org/10.1016/j.agrformet.2014.03.003>.
- Campbell D.I., Wall A.M., Nieveen J.P., Schipper L.A. (2015). Variations in CO<sub>2</sub> exchange for dairy farms with year-round rotational grazing on drained peatlands. *Agric. Ecosyst. Environ.* V.202, pp.68–78. <http://dx.doi.org/10.1016/j.agee.2014.12.019>.
- Ciais P., Sabine C., Bala, G., Bopp, L., Brovkin, V., Canadell, J., Chhabra, A., DeFries, R., Galloway, J., Heimann, M., Jones, C., Le Quéré, C., Myneni, R.B., Piao, S., Thornton, P. (2013). Carbon and Other Biogeochemical Cycles. In: *Climate Change 2013: The Physical Science Basis. Contribution of Working Group I to the Fifth Assessment Report of the Intergovernmental Panel on Climate Change* [Stocker, T.F., Qin, D., Plattner, G.-K., Tignor, M., Allen, S.K., Boschung, J., Nauels, A., Xia, Y., Bex, V., Midgley, P.M. (eds.)]. Cambridge University Press, Cambridge, United Kingdom and New York, NY, USA.
- Davydov D.K., Dyachkova A.V., Fofonov A.V., Maksyutov S.S., Dyukarev E.A., Smirnov S.V., Glagolev M.V. (2018). Measurements of methane and carbon dioxide fluxes from wetland ecosystems of the Southern Taiga of West Siberia. *Proceedings of SPIE - The International Society for Optical Engineering*. V.10833, 1083389.
- Dyukarev E.A. (2017). Partitioning of net ecosystem exchange using chamber measurements data from bare soil and vegetated sites. *Agricultural and Forest Meteorology*. V.239, pp. 236–248. <https://doi.org/10.1016/j.agrformet.2017.03.011>.
- Dyukarev E.A., Golovatskaya E.A., Duchkov A.D., Kazantsev S.A. (2009). Temperature monitoring in Bakchar bog (West Siberia). *Russian Geology and Geophysics*, N.6, pp. 745–754. <https://doi.org/10.1016/j.rgg.2008.08.010>.

Dyukarev E.A., Pologova N.N., Dyukarev A.G., Golovatskaya E.A. (2011). Forest cover disturbances in the South Taiga of Western Siberia. *Environ. Res. Lett.* V.6, N.3, 035203 9pp. <https://doi.org/10.1088/1748-9326/6/3/035203>.

Eckhardt T., Knoblauch C., Kutzbach L., Simpson G., Abakumov E., and Pfeiffer E.-M. (2018). Partitioning CO<sub>2</sub> net ecosystem exchange fluxes on the microsite scale in the Lena River Delta, Siberia, *Biogeosciences Discuss.*, <https://doi.org/10.5194/bg-2018-311>, in review.

Falge E., Baldocchi D., Olson R., Anthoni P., Aubinet M., Bernhofer C., Burba G., Ceulemans R., Clement R., Dolman H., Granier A., Gross P., Grünwald T., Hollinger D., Jensen N.-O., Katul G., Keronen P., Kowalski A., Ta Lai C., Law B.E., Meyers T., Moncrieff J., Moors E., Munger J.W., Pilegaard K., Rannik Ü., Rebmann C., Suyker A., Tenhunen J., Tu K., Verma S., Vesala T., Wilson K., Wofsy S. (2001). Gap filling strategies for defensible annual sums of net ecosystem exchange. *Agric. For. Meteorol.* V.107, pp.43–69. [https://doi.org/10.1016/S0168-1923\(00\)00225-2](https://doi.org/10.1016/S0168-1923(00)00225-2).

Filippova N.V., Bulyonkova T.M., Lapshina, E.D. (2015). Fleshy fungi forays in the vicinities of the YSU Mukhrino field station (Western Siberia). *Environ. Dyn. Glob. Clim. Change*, V.6, pp.3–31. <http://dx.doi.org/10.17816/edgcc613-31>.

Fleischer E., Khashimov I., Hölzel N., Klemm O. (2016). Carbon exchange fluxes over peatlands in Western Siberia: Possible feedback between land-use change and climate change. *Science of the Total Environment*. V.545–546, pp. 424–433. <https://doi.org/10.1016/j.scitotenv.2015.12.073>.

Franz D., Acosta M., Altimir N., Arriga N., Arrouays D., Aubinet M. et al. (2018). Towards long-term standardised carbon and greenhouse gas observations for monitoring Europe's terrestrial ecosystems: a review. *International Agrophysics*. V.32, N.4, pp. 439-455. <https://doi.org/10.1515/intag-2017-0039>.

Glagolev M., Kleptsova I., Filippov I., Maksyutov S., Machida T. (2011). Regional methane emission from West Siberia mire landscapes. *Environ. Res. Lett.*, V.6, pp. 045214, <https://doi.org/10.1088/1748-9326/6/4/045214>.

Glagolev M.V., Ilyasov D.V., Terentyeva I.E., Sabrekov A.F., Krasnov O.A., Maksyutov Sh.Sh. (2017). Methane and carbon dioxide fluxes in the waterlogged forests of Western Siberian southern and middle taiga subzones. *Optika Atmosfery i Okeana*. V.30, N. 04, pp. 301–309 (in Russian).

Golovatskaya E.A., Dyukarev E.A. (2011). Seasonal and diurnal dynamics of CO<sub>2</sub> emission from oligotrophic peat soil surface. *Russian Meteorology and Hydrology*. N.6, pp.84-93. <https://link.springer.com/article/10.3103%2FS1068373911060094>.

Golovatskaya E.A. and Dyukarev E.A. (2012). The influence of environmental factors on the CO<sub>2</sub> emission from the surface of oligotrophic peat soils in West Siberia. *Eurasian Soil Science Journal*. N.6, pp. 658–667. <https://link.springer.com/article/10.1134/S106422931206004X>.

Golovatskaya E.A., Dyukarev E.A., Ippolitov I.I., Kabanov M.V. (2008). Influence of landscape and hydrometeorological conditions on CO<sub>2</sub> emission in peatland ecosystems. *Doklady Earth Sciences*. N.4, pp.1-4.

Grant R.F., Desai A.R., Sulman B.N. (2012). Modelling contrasting responses of wetland productivity to changes in water table depth. *Biogeosciences*, V.9, N.11, pp.4215–4231. <https://doi.org/10.5194/bg-9-4215-2012>.

Grebenyuk G.N., Kuznetsova V.P. (2012). Modern climate dynamics and phenological variability of northern territories. *Fundamental research*, N.11-5, pp. 1063-1077 (in Russian).

Günther A., Jurasinski G., Albrecht K., Gaudig G., Krebs M., Glatzel S. (2017) Greenhouse gas balance of an establishing Sphagnum culture on a former bog grassland in Germany. *Mires and Peat*. V.20, pp. 1-16. <https://doi.org/10.19189/MaP.2015.OMB.210>.

Helfter C., Campbell C., Dinsmore K.J., Drewer J., Coyle M., Anderson M., Skiba U., Nemitz E., Sutton M.A. (2015). Drivers of long-term variability in CO<sub>2</sub> net ecosystem exchange in a temperate peatland. *Biogeosciences*, V.12, N.6, pp.1799–1811. <https://doi.org/10.5194/bg-12-1799-2015>.

Humphreys E.R., Lafleur P.M. (2011). Does earlier snowmelt lead to greater CO<sub>2</sub> sequestration in two low arctic tundra ecosystems? *Geophys. Res. Lett.* V.38, N.5, L09703. <https://doi.org/10.1029/2011GL047339>.

Ivanov D.G., Avilov V.K., Kurbatova Y.A. (2017). CO<sub>2</sub> fluxes at south taiga bog in the European part of Russia in summer. *Contemporary Problems of Ecology*. V.10, N.2, pp. 97–104. <https://doi.org/10.1134/s1995425517020056>.

Kabanov M.V. (2015). Regional climate-regulating factors in Western Siberia *Geography and Natural Sciences*. V.3, pp. 207-113.

Kandel T.P., Elsgaard L., Larke, P.E. (2013). Measurement and modelling of CO<sub>2</sub> flux from a drained fen peatland cultivated with reed canary grass and spring barley. *GCB Bioenergy*. V.5, pp. 548-561. <https://doi.org/10.1111/gcbb.12020>.

Kurbatova J., Li C., Tatarinov F., Varlagin A., Shalukhina N., Olchev A. (2009). Modeling of the carbon dioxide fluxes in European Russia peat bogs. *Environmental Research Letters*, V.4, N.4, 045022. <https://doi.org/10.1088/1748-9326/4/4/045022>.

Kurganova I.N., Lopes de Gerenyu V.O. L., Petrov A.S., Myakshina T.N., Sapronov D.V., Ableeva V. A., Kudryarov V. N. (2011). Effect of the observed climate changes and extreme weather phenomena on the emission component of the carbon cycle in different ecosystems of the southern taiga zone. *Doklady Biological Sciences*, V.441, N.1, pp. 412-416. <https://doi.org/10.1134/S0012496611060214>.

Lagarias J.C., Reeds J.A., Wright M.H., Wright P.E. (1998). Convergence properties of the nelder-mead simplex method in low dimensions. *SIAM Journal of Optimization*, V.9, N.1, pp. 112–147.

Laine A., Riutta T., Juutinen S., Valiranta M., Tuittila E.S. (2009). Acknowledging the spatial heterogeneity in modelling/reconstructing carbon dioxide exchange in a northern aapa mire. *Ecol. Modell.* V.220, pp.2646–2655. <https://doi.org/10.1016/j.ecolmodel.2009.06.047>.

Laine A.M., Mehtätalo L., Tolvanen A., Froking S., Tuittila E.S. (2019). Impacts of drainage, restoration and warming on boreal wetland greenhouse gas fluxes *Sci. Total Environ.*, V.647 pp. 169-181, <https://doi.org/10.1016/j.scitotenv.2018.07.390>.

Lapshina E.D., Alexeychik P., Dengel S., Filippova N.V., Zarov E.A., Filippov I.V., Terentyeva I.E., Sabrekov A.F., Solomin Y.R., Karpov D.V., Mammarella I. (2015). A new peatland research station in the center of West Siberia: description of infrastructure and research activities. *Report series in aerosol science*. pp. 236-240. <http://www.atm.helsinki.fi/faar/reportseries/rs-180.pdf>.

Leifeld J., Menichetti L. (2018). The underappreciated potential of peatlands in global climate change mitigation strategies, *Nat. Commun.*, V.9, pp.1071, <https://doi.org/10.1038/s41467-018-03406-6>.

Leroy F., Gogo S., Guimbaud C., Bernard-Jannin L., Hu Z., Laggoun-Défarge F. (2017). Vegetation composition controls temperature sensitivity of CO<sub>2</sub> and CH<sub>4</sub> emissions and DOC concentration in peatlands. *Soil Biology and Biochemistry*, V.107, pp.164–167. <https://doi.org/10.1016/j.soilbio.2017.01.005>.

Mäkelä A., Hari P., Berninger F., Hänninen H., Nikinmaa E. (2004). Acclimation of photosynthetic capacity in Scots pine to the annual cycle of temperature. *Tree Physiol.* V.24, N.4, pp. 369–376. <https://www.ncbi.nlm.nih.gov/pubmed/14757576>.

McVeigh P., Sottocornola M., Foley N., Leahy P., Kiely G. (2014). Meteorological and functional response partitioning to explain interannual variability of CO<sub>2</sub> exchange at an Irish Atlantic blanket bog. *Agricultural and Forest Meteorology* V.194, pp. 8–19. <https://doi.org/10.1016/j.agrformet.2014.01.017>.

Minkkinen K., Ojanen P., Penttilä T., Aurela M., Laurila T., Tuovinen J.-P., Lohila A. (2018). Persistent carbon sink at a boreal drained bog forest. *Biogeosciences*. V.15, N.11, pp. 3603–3624. <https://doi.org/10.5194/bg-15-3603-2018>.

Molchanov A.G. (2015). Gas exchange in sphagnum mosses at different near-surface groundwater levels. *Russian Journal of Ecology*. V.46, N.3. pp. 230-235. <https://doi.org/10.7868/s0367059715030063>.

Molchanov A.G., Olchev A.V. (2016) Model of CO<sub>2</sub> exchange in a sphagnum peat bog. *Computer research and modelling*. V.8. N.2. pp. 369-377.

Munir T.M., Xu B., Perkins M., Strack M. (2014). Responses of carbon dioxide flux and plant biomass to water table drawdown in a treed peatland in Northern Alberta: A climate change perspective. *Biogeosciences*. V.11, N.3, pp. 807–820. <https://doi.org/10.5194/bg-11-807-2014>.

Naumov A.V. (2009). Soil respiration. Novosibirsk, Izd SO RAN. P. 208.

Nilsson M., Sagerfors J., Buffam I., Laudon H., Eriksson T., Grelle A., Klemetsson L., Weslien P., Lindroth A. (2008). Contemporary carbon accumulation in a boreal oligotrophic minerogenic mire – a significant sink after accounting for all C-fluxes. *Global Change Biol.* 14 (10), 2317–2332. <https://doi.org/10.1111/j.1365-2486.2008.01654.x>.

Olefeldt D., Roulet N.T., Bergeron O., Crill P., Bäckstrand K., Christensen T.R. (2012). Net carbon accumulation of a high-latitude permafrost tundra mire similar to permafrost-free peatlands. *Geophys. Res. Lett.* 39, L03501 <https://doi.org/10.1029/2011GL050355>.

Olchev A., Novenko E., Desherevskaya O., Krasnorutskaya K., Kurbatova J. (2009). Effects of climatic changes on carbon dioxide and water vapor fluxes in boreal forest ecosystems of European part of Russia. *Environmental Research Letters*, V.4, N.4, 045007 <https://doi.org/10.1088/1748-9326/4/4/045007>.

Page S., Baird A. (2016). Peatlands and global change: response and resilience, *Ann. Rev. Environ. Resour.*, V.41, pp.35–57.

Parazoo N.C., Koven C.D., Lawrence D.M., Romanovsky V. Miller C.E. (2017) Detecting the permafrost carbon feedback: Talik formation and increased cold-season respiration as precursors to sink-to-source transitions. *The Cryosphere*, <https://doi.org/10.5194/tc-2017-189>.

Pavelka M., Acosta M., Kiese R., Altimir N., Brümmer C., Crill P., Darenova E., Fuß R., Gielen B., Graf A., Klemedtsson L., Lohila A., Longdoz B., Lindroth A., Nilsson M., Jiménez S., Merbold L., Montagnani L., Peichl M., Pihlatie M., Pumpanen J., Ortiz P., Silvennoinen H., Skiba U., Vestin P., Weslien P., Janous D., Kutsch, W. (2018). Standardisation of chamber technique for CO<sub>2</sub>, N<sub>2</sub>O and CH<sub>4</sub> fluxes measurements from terrestrial ecosystems. *International Agrophysics*, V.32, N.4, pp.569–587. <https://doi.org/10.1515/intag-2017-0045>.

Peatlands of West Siberia (1976). Their composition and hydrological regime. Leningrad, Hydrometeoizdat. P. 615.

Pessarakli M. (2005). *Handbook of Photosynthesis*. Taylor & Francis Group. P.928.

Pugh C. A., Reed D. E., Desai A. R., Sulman B. N. (2018). Wetland flux controls: how does interacting water table levels and temperature influence carbon dioxide and methane fluxes in northern Wisconsin? *Biogeochemistry*, V.137, N.1–2, pp. 15–25. <https://doi.org/10.1007/s10533-017-0414-x>.

Ratcliffe J.L., Creevy A., Andersen R., Zarov E., Gaffney P., Taggart M.A., Mazei Y., Tsyganov A.N., Rowson J.G., Lapshina E.D., Payne R.J. (2017). Ecological and environmental transition across the forested-to-open bog ecotone in a west Siberian peatland *Science of the Total Environment*. V.607-608, pp.816-828. <https://doi.org/10.1016/j.scitotenv.2017.06.276>.

Runkle B.R.K., Sachs T., Wille C., Pfeiffer E.-M., Kutzbach L. (2013). Bulk partitioning the growing season net ecosystem exchange of CO<sub>2</sub> in Siberian tundra reveals the seasonality of its carbon sequestration strength. *Biogeosciences*. V.10, pp.1337-1349. <https://doi.org/10.5194/bg-10-1337-2013>, 2013.

Rydin H., Jeglum J. (2015). *The Biology of Peatlands*. Oxford. Univ. Press., pp. 400.

Sasakawa M., Ito A., Machida T., Tsuda N., Niwa Y., Davydov D., Fofonov A., Arshinov M. (2012). Annual variation of CH<sub>4</sub> emissions from the middle taiga in West Siberian Lowland (2005-2009): A case of high CH<sub>4</sub> flux and precipitation rate in the summer of 2007. *Tellus, Series B: Chemical and Physical Meteorology*, V.64, N.1, pp.1–10. <https://doi.org/10.3402/tellusb.v64i0.17514>.

Saunois M., Bousquet P., Poulter B., Peregon A., Ciais P., Canadell J. G., Dlugokencky E. J., Etiope G., Bastviken D., Houweling S., Janssens-Maenhout G., Tubiello F. N., Castaldi S., Jackson R. B., Alexe M., Arora V. K., Beerling D. J., Bergamaschi P., Blake D. R., Brailsford G., Brovkin V., Bruhwiler L., Crevoisier C., Crill P., Covey K., Curry C., Frankenberg C., Gedney N., Höglund-Isaksson L., Ishizawa M., Ito A., Joos F., Kim H.-S., Kleinen T., Krummel P., Lamarque J.-F., Langenfelds R., Locatelli R., Machida T., Maksyutov S., McDonald K. C., Marshall J., Melton J. R., Morino I., Naik V., O'Doherty S., Parmentier F.-J.W., Patra P. K., Peng C., Peng S., Peters G. P., Pison I., Prigent C., Prinn R., Ramonet M., Riley W. J., Saito M., Santini M., Schroeder R., Simpson I. J., Spahn R., Steele P., Takizawa A., Thornton B. F., Tian H., Tohjima Y., Viovy N., Voulgarakis A., van Weele M., van der Werf G. R., Weiss R., Wiedinmyer C., Wilton D. J., Wiltshire A., Worthy D., Wunch D., Xu X., Yoshida Y., Zhang B., Zhang Z., Zhu Q. (2016). The global methane budget 2000–2012, *Earth Syst. Sci. Data*, V.8, pp.697-751. <https://doi.org/10.5194/essd-8-697-2016>.



Sheng Y., Smith L.C., MacDonald G.M., Kremenetski K.V., Frey K.E., Velichko A.A., Lee M., Beilman D.W., Dubinin P. (2004). A high-resolution GIS-based inventory of the west Siberian peat carbon pool. *Global Biogeochemical Cycles*. V.18, p.GB3004.

Sokolov A.V., Mamkin V.V., Avilov V.K., Tarasov D.L., Kurbatova J.A., Olchev A.V. (2019). Application of a balanced identification method for gap-filling in CO<sub>2</sub> flux data in a sphagnum peat bog. *Computer research and modelling*. V.11, N.1, pp.153-171. <https://doi.org/10.20537/2076-7633-2019-11-1-153-171>.

Stepanova V.A., Pokrovsky O.S. (2011). Macroelement composition of raised bogs peat in the middle taiga of Western Siberia (the bog complex Mukhrino), Tomsk State University Bulletin. V.352, pp.211–214, (in Russian).

Swenson M.M., Regan S., Bremmers D.T.H., Lawless J., Saunders M., Gill L.W. (2019). Carbon balance of a restored and cutover raised bog: implications for restoration and comparison to global trends. *Biogeosciences*. V.16, pp.713-731, <https://doi.org/10.5194/bg-16-713-2019>.

Szajdak L.W., Lapshina E.D., Gaca W., Styla K., Meysner T., Szczepanski M., Zarov E.A. (2016). Physical, chemical and biochemical properties of Western Siberia Sphagnum and Carex peat soils, *Environ. Dyn. Glob. Clim. Change*, V.7, pp. 13–25. <http://dx.doi.org/10.17816/edgcc7213-25>

Taylor N., Price J., Strack M. (2016). Hydrological controls on productivity of regenerating Sphagnum in a cutover peatland. *Ecohydrology*, V.9, N.6, pp. 1017–1027. <https://doi.org/10.1002/eco.1699>.

Terentjeva I. E., Glagolev M. V., Lapshina E. D., Sabrekov A. F., Maksyutov S. (2016). Mapping of West Siberian taiga wetland complexes using Landsat imagery: implications for methane emissions, *Biogeosciences*, V.13, pp.4615–4626, <https://doi.org/10.5194/bg-13-4615-2016>.

The second assessment report of Roshydromet on climate change and their consequences on the territory of the Russian Federation (2014). Federal service for Hydrometeorology and environmental monitoring. pp. 605.

Veretennikova E.E. and Dyukarev E.A. (2017). Diurnal variations in methane emissions from West Siberia peatlands in summer. *Russian Meteorology and Hydrology*. V.42, N.5, pp. 319-326. <https://link.springer.com/article/10.3103/S1068373917050077>.

Vomperskiy S.E. (1994). The role of peatlands in carbon cycling, in *Biogeocenotic features of peatlands and their rational exploitation*. Moscow, Nauka, pp. 5-37.

Walker T.N., Garnett M.H., Ward S.E., Oakley S., Bardgett R. D., Ostle N. J. (2016). Vascular plants promote ancient peatland carbon loss with climate warming. *Global Change Biology*, V.22, N.5, pp. 1880–1889. <https://doi.org/10.1111/gcb.13213>.

Webster K.L., Bhatti J.S., Thompson D.K., Nelson S.A., Shaw C.H., Bona K.A., Hayne S.L., Kurz W.A. (2018). Spatially-integrated estimates of net ecosystem exchange and methane fluxes from Canadian peatlands. *Carbon Balance and Management*, V.13, N.1. <https://doi.org/10.1186/s13021-018-0105-5>.

Widlowski J.-L., Pinty B., Clerici M., Dai Y., De Kauwe M., de Ridder K., Kallel A., Kobayashi H., Lavergne T., NiMeister W., Olchev A., Quaife T., Wang S., Yang W., Yang Y., Yuan H. (2011). RAMI4PILPS: An intercomparison of formulations for the partitioning of solar radiation in land surface models. *Journal of Geophysical Research: Biogeosciences*, V.116, N.2. <https://doi.org/10.1029/2010JG001511>.

Wu J., Roulet N.T., Moore T.R., Lafleur P., Humphreys E. (2010). Dealing with microtopography of an ombrotrophic bog for simulating ecosystem-level CO<sub>2</sub> exchanges. *Ecological Modelling*. V.222, N.4, pp. 1038–1047. <https://doi.org/10.1016/j.ecolmodel.2010.07.015>.

Yurova A., Wolf A., Sagerfors J., Nilsson M. (2007). Variations in net ecosystem exchange of carbon dioxide in a boreal mire: Modeling mechanisms linked to water table position. *Journal of Geophysical Research: Biogeosciences*, V.112, N.2, G02025. <https://doi.org/10.1029/2006JG000342>.

Zhaojun B., Joosten H., Hongkai L., Gaolin Z., Xingxing Z., Jinze M., Jing Z. (2011). The response of peatlands to climate warming: A review. *Acta Ecologica Sinica*, V.31, N.3, pp.157–162. <https://doi.org/10.1016/j.chnaes.2011.03.006>.

Zhou L., Zhou G., Jia Q. (2009). Annual cycle of CO<sub>2</sub> exchange over a reed (*Phragmites australis*) wetland in Northeast China. *Aquatic Botany*, V.91, N.2, pp. 91–98. <https://doi.org/10.1016/j.aquabot.2009.03.002>.

Zhu X., Song C., Swarenzenski C.M., Guo Y., Zhang X., Wang J. (2015). Ecosystem-atmosphere exchange of CO<sub>2</sub> in a temperate herbaceous peatland in the Sanjiang Plain of northeast China. *Ecological Engineering*, V.75, pp. 16–23. <https://doi.org/10.1016/j.ecoleng.2014.11.035>.

Received on Dec 16<sup>th</sup> 2018

Accepted on May 17<sup>th</sup>, 2019